Adsorption of Glucose into Zeolite Beta from Aqueous Solution

Peng Bai and J. Ilja Siepmann
Dept. of Chemistry, and Chemical Theory Center, University of Minnesota, Minneapolis, MN 5545

Depts. of Chemistry and of Chemical Engineering and Materials Science and Chemical Theory Center, University of Minnesota, Minneapolis, MN 55455

Michael W. Deem
Dept. of Bioengineering, Rice University, Houston, TX 77005

Dept. of Physics and Astronomy, Rice University, Houston, TX 77005

DOI 10.1002/aic.14104
Published online April 16, 2013 in Wiley Online Library (wileyonlinelibrary.com)

Hydrophobic zeolites, including Ti- and Sn-beta, have been found to adsorb and isomerize glucose into fructose. An experimental question has been the significance of the entropic contribution to the free energy of transfer of glucose from solution to zeolite. We here perform Gibbs ensemble Monte Carlo calculations to quantify the enthalpy, entropy, and free energy of transfer of glucose from the aqueous phase to the zeolite phase. We find that the entropic contribution is large and positive, nearly compensating for an unfavorable enthalpy of transfer in all-silica zeolite beta. A significant component of the positive entropy of transfer from the aqueous phase to zeolite is the unstructuring of first coordination shell waters around glucose as it leaves the solution. *AIChE J*, 59: 3523-3529, 2013
Keywords: adsorption/liquid, computer simulations (MC and MD), materials

Introduction

Zeolites are nanoporous crystals, classically with chemical composition $Si_{1-x}Al_xO_2$. The first zeolite to be commercialized was Linde type A in 1953,[1] and zeolites are now widely used in catalytic, sorption, and separation processes.[2] Tuning of the shape selectivity that results from different pore architectures is a fundamental principle in the field of zeolite catalysis.[3] An interesting subset of zeolites are the hydrophobic zeolites, first prepared in 1978.[4,5] These materials can adsorb and react on hydrophobic compounds in aqueous phase. The (nearly) water-free environment provided by hydrophobic zeolite frameworks allows catalysis of different reactions than does aqueous media or the environment of hydrophilic zeolites.[6,7] That is, these defect-free hydrophobic zeolites allow catalysis that would otherwise be poisoned in the presence of water in the zeolite host. Hydrophobic zeolites similarly provide unique catalytic pathways to react on compounds in two-phase water-organic mixtures, as might occur during conversion of biomass feed stocks.[8–11]

A particularly interesting transformation that illustrates the properties of hydrophobic zeolites is the isomerization of glucose into fructose in these materials.[7,12–14] In contrast, in zeolites with defects and which are not hydrophobic, adsorbed water molecules inhibit the Lewis-acid-catalyzed isomerization. Interestingly, the mechanism of isomerization in hydrophobic zeolites follows a pathway quite similar to that of metalloenzyme-catalyzed isomerization.[15] It appears that the hydrophobic zeolite provides a water-excluded region for the catalysis to occur, just as the hydrophobic groups in the metalloenzyme do. In addition to hydrophobicity of the zeolite, a good match between pore size and substrate size is also important for catalytic yield and conversion.[13]

The first step of zeolite-catalyzed isomerization of glucose is the transfer of glucose from the aqueous phase to the zeolite phase. A natural question, not yet answered experimentally, is to what extent there is an entropic driving force for this partitioning. We wonder, in particular, whether there is a restructuring of the water as the glucose leaves the aqueous phase. The effect of this restructuring would be primarily entropic in nature. We here quantify the contribution of this water restructuring to the free energy of transfer for glucose from the aqueous phase to zeolite beta (designated as BEA framework). These calculations complement recent experimental studies of this transformation in zeolite beta.[16]

The remainder of this article is organized as follows. In the Methods section, we discuss the molecular models and Monte Carlo algorithms used to calculate thermodynamic and structural properties. In the Results and Discussion section, we give results for the enthalpy, entropy, and free energy of transfer of glucose to zeolite beta and discuss structural properties. We discuss the importance of water restructuring on the driving force for adsorption of glucose within zeolite beta from aqueous solution. We conclude in the final section.

Correspondence concerning this article should be addressed to M. W. Deem at mwdeem@rice.edu.

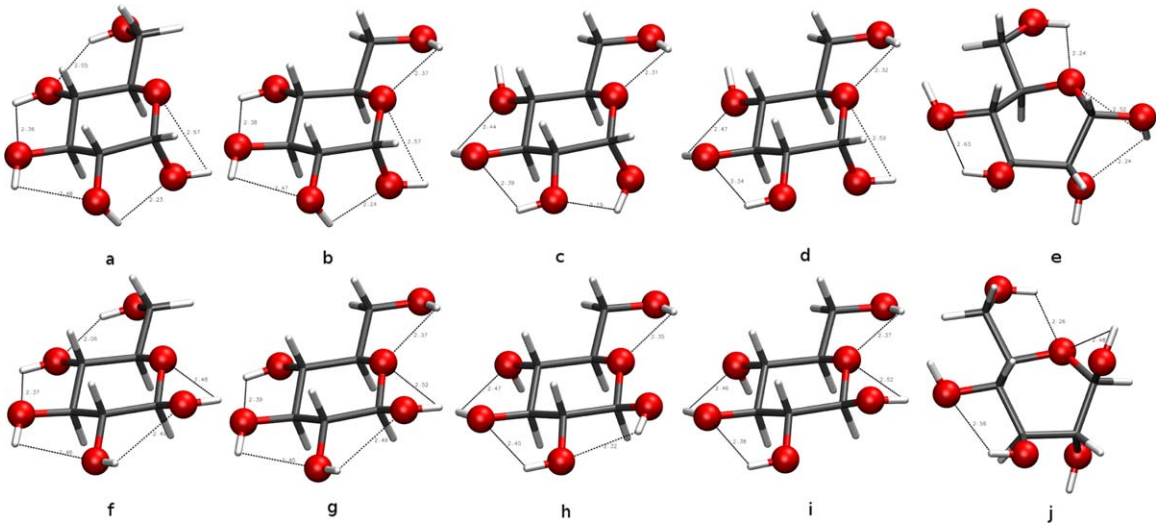

Figure 1. Locally optimized conformations of glucose: (a) and (b), two forms of the α-chair with counter clockwise hydrogen bonding pattern; (c) and (d), two forms of the α-chair with clockwise hydrogen bonding pattern; (e), α-boat; (f) and (g), two forms of the β-chair with counter clockwise hydrogen bonding pattern; (h) and (i), two forms of the β-chair with clockwise hydrogen bonding pattern; (j), β-boat.

[Color figure can be viewed in the online issue, which is available at wileyonlinelibrary.com.]

Methods

Zeolite beta is an intergrown hybrid of two closely related polymorphs that both possess a fully three-dimensional pore structure with 12-ring as the windows between cages. Polymorph A forms an enantiomorphic pair with space group symmetries $P4_122$ and $P4_322$, with $a = 1.266$ nm and $c = 2.641$ nm. In this simulation study, we used $3 \times 3 \times 2$ unit cells of the all-silica polymorph A with the structure determined by Newsam et al.,[17] that is, the simulation box lengths are 3.798 and 5.282 nm, respectively, and it contains 3456 framework atoms with interaction sites placed at both O and Si locations. The all-silica zeolite beta structure is treated as rigid, and the simulation box is periodically replicated in all three directions to form an infinite sorbent structure without open surfaces.

The sorbent–sorbate and sorbate–sorbate intermolecular interactions are described using Lennard–Jones 12–6 (LJ) and Coulomb potentials, with parameters taken from the TIP4P (Transferable Intermolecular Potential 4 Point) model[18] for water, the OPLS-AA (Optimized Potentials for Liquid Simulations – All Atom) force field for glucose,[19] and the TraPPE-zeo (Transferable Potentials for Phase Equilibria – zeolite) force field[20,21] for the framework atoms. For the TraPPE-zeo force field, a training set of sorption isotherms for alkanes, carbon dioxide, and ethanol was used for the parameterization of the interaction sites in the zeolite matrix. The glucose molecule is modeled as semiflexible with a rigid ring structure and flexible hydroxyl groups and side chain. The LJ parameters for all unlike interactions, including those with zeolite framework atoms, are obtained using Lorentz–Berthelot combining rules. A spherical potential truncation at a distance of 1.4 nm is used for sorbate–sorbate interactions and for those in the solution phase with analytical tail corrections to estimate LJ interactions beyond this distance.[22] Coulomb interactions are treated using the Ewald summation method.[22] All host–guest interactions are pretabulated and interpolated during simulation.[23]

The MCCCS-MN (Monte Carlo for Complex Chemical Systems – Minnesota) software[24] was used for all Monte Carlo (MC) simulations. The adsorption equilibria were determined using the isobaric–isothermal version of the Gibbs ensemble[25] with three simulation boxes used to represent the zeolite phase, the solution phase, and a vapor-phase transfer medium. This setup is very similar to those previously used by us to study liquid–liquid equilibria,[26] retention in reversed-phase liquid chromatography,[27] and adsorption of methanol and ethanol onto silicalite-1 from aqueous solution.[20] The Gibbs ensemble simulations were performed using a system size consisting of 1000 water molecules at the three different compositions of 9, 18, and 36 glucose molecules per 1000 water molecules; the three temperatures of 348 K, 353 K, and 358 K; and an external pressure of 1 atm. In addition to conventional translational, rotational, and volume moves, we used two types of configurational-bias Monte Carlo (CBMC) moves: coupled-decoupled CBMC swap moves that transfer particles (only water and the smallest glucose intermediate) between different simulation boxes[28–31] and CBMC identity switch moves that convert between two related molecules.[32] Because cavities of the size needed to accommodate a glucose molecule do not appear with sufficient frequency in liquid water, the transfer of glucose molecules is enhanced through multiple intermediate glucose variants that have scaled interactions and an external biasing potential is used to help with the transfer of glucose variants to the vapor phase (and corrected for in the calculation of the transfer-free energies).[33] The probabilities for performing both types of the CBMC transfer moves were adjusted so that about one move of each type was accepted per 10 MC cycles. Sixteen independent simulations were carried out at each state point. The equilibration and production periods consisted of 100,000–250,000 and 100,000 MC cycles, respectively, where each cycle consists of N MC trial moves.

In addition to the Gibbs ensemble Monte Carlo (GEMC) simulations for the adsorption equilibria, additional simulations were carried out in the isobaric–isothermal ensemble[34] to quantify the enthalpy of solvation for glucose in water. To this extent, an isolated gas-phase glucose molecule and liquid phases consisting of either 1000 water molecules or of one glucose and 1000 water molecules were studied.

Table 1. Energy of D-Glucose Conformers in kJ/mol Relative to Conformer a

a	b	c	d	e	f	g	h	i	j
0	0.06	8.12	15.62	43.58	5.09	4.70	19.78	22.55	46.17

Results and Discussion

As aforementioned, for computational efficiency a semi-rigid glucose model was used for this work. Thus, the first task was to identify the ring structure that is energetically most favorable. To this extent, electronic structure calculations using Kohn–Sham density functional theory with the M06-2X/6–311+g(3df,3pd) combination of functional and basis set[35] were used. Figure 1 illustrates the gas-phase-optimized structures and Table 1 summarizes the corresponding energies. Conformers **a** and **b** are significantly lower in energy than the other conformers and their geometries for the six ring atoms and for those six atoms directly bonded to the ring are very similar. Thus, the 12-atom core from the **a** conformer is used to initialize the simulations. Because the hydroxyl groups and the side chain can freely rotate, Conformers **a–d**, that is, the α chair structures, are allowed in the simulation. It should be noted that Conformers **f** and **g** are also within the thermally accessible energy range, but are inaccessible in the simulations. Given the similarity of the overall shapes, it is likely that the adsorption and solvation behavior for Conformers **a** and **f** (and conformers **b** and **g**) would be quite similar. A question that cannot be answered with the current simulation protocol is whether the population of the open-chain form would be significant in zeolite beta. The lengths of the intramolecular hydrogen bonds are also indicated in Figure 1, and with the exception of the one hydrogen bond of Conformer **a** involving the hydroxyl group of the CH_2OH group as donor, all other intramolecular hydrogen bonds are longer than 0.22 nm, that is, fairly strained.

In GEMC simulations of multicomponent adsorption systems, only the overall composition is specified, and molecules distribute between the different phases through particle transfer moves.[36] Within the statistical errors, the partition coefficients are found to agree for all three temperatures. The simulations containing a total of 9, 18, and 36 glucose molecules yield weight fractions of 0.05, 0.09, and 0.17, respectively, in the aqueous phase. The corresponding loadings for glucose in the zeolite are 0.17 ± 0.03, 0.32 ± 0.05, and 0.46 ± 0.04 molecules per crystallographic unit cell, respectively, that is, they exhibit a linear correlation with the solution-phase concentrations. In contrast, the corresponding loadings for water in the zeolite are 0.49 ± 0.08, 0.68 ± 0.12, and 0.83 ± 0.15 molecules per crystallographic unit cell, respectively. As was also found for mixtures of primary alcohols and water,[20] the adsorption of glucose induces coadsorption of water. A nearly linear relation exists between adsorbed water and adsorbed glucose, $n^{\mathrm{ads}}_{\mathrm{water}} \approx 0.30 + 1.2 \times n^{\mathrm{ads}}_{\mathrm{glucose}}$.

The Gibbs free energy of transfer from Phase **A** to Phase **B** can be evaluated directly from the ratio of number densities as follows[37]

$$\Delta G_{\mathrm{trans}} = -RT \ln \frac{\rho_{\mathbf{B}}}{\rho_{\mathbf{A}}}$$

where $\rho_{\mathbf{A}}$ and $\rho_{\mathbf{B}}$ are the number densities of the solute in the two phases. Due to the relatively small number of successful complete particle transfers, we used data from all nine state points to estimate $\Delta G_{\mathrm{trans}}$ and found values of $+42$ and $+2.2$ kJ/mol for the transfer from the aqueous phase to the vapor and to the zeolite phase, respectively. As can be seen, the transfer into the zeolite phase is significantly more favorable than the transfer to the vapor phase. In our GEMC simulations, both the glucose and the water molecules are allowed to transfer between all three phases. The fluctuating particle numbers resulting from the phase transfers make a direct estimation of the enthalpy of transfer, a statistically very challenging problem;[38] hence, separate simulations with fixed numbers of particles in the isobaric–isothermal ensemble were used to compute the enthalpy of transfer at infinite dilution. The numerical data are summarized in Table 2. The potential energies for all three systems increase monotonically with temperature, but as the enthalpy of solvation for transfer from vapor phase to solution phase involves computing a small number from the difference of two larger numbers, larger by about two orders of magnitude, the uncertainty in ΔH_{sol} is larger than the temperature effect. Averaging over all three temperatures, we estimate $\Delta H_{\mathrm{trans}} = -\Delta H_{\mathrm{sol}} = 141 \pm 6$ kJ/mol. As will be seen from the structural analysis provided below, the solvation structure around the glucose molecules and the number of hydrogen bonds formed to the solvent do not show a significant concentration dependence over the range of state points investigated here.

Once the Gibbs free energy and the enthalpy of transfer are known, the entropy of transfer can be estimated from the usual thermodynamic definition

$$\Delta G_{\mathrm{trans}} = \Delta H_{\mathrm{trans}} - T\Delta S_{\mathrm{trans}}$$

As is already clear from the different magnitudes of $\Delta G_{\mathrm{trans}}$ and $\Delta H_{\mathrm{trans}}$ for the transfer of glucose from the aqueous phase to the vapor phase, the entropy of transfer must be large and positive, and a value of $+280 \pm 20$ J/(mol K) is estimated here.

The numerical data for the energetics of the adsorption process are summarized in Table 3. Because the temperature effects are minor (see below) and statistically significant differences were not observed, the data are averaged over the three temperatures. The potential energies of glucose and of water in the zeolite increase slightly in magnitude with increasing glucose concentration, that is, sorbate–sorbate interactions play a minor role at the compositions investigated here. The magnitude of the potential energy for glucose in the zeolite appears quite large at first glance, but it should be noted that the intramolecular energy for glucose in the vapor phase is also large and negative (see Table 2). The values of the potential energy of glucose in the zeolite and

Table 2. Potential Energies and Enthalpies of Solvation in kJ/(mol of System) at Three Temperatures

		Temperature		
System	Property	348 K	353 K	358 K
Isolated glucose molecule	U	-295.3 ± 0.4	-295.0 ± 0.2	-294.8 ± 0.3
1000 water molecules	U	-38394 ± 7	-38096 ± 7	-37794 ± 9
1 glucose + 1000 water molecules	U	-38821 ± 5	-38532 ± 11	-38230 ± 8
Solvation	ΔH_{sol}	-135 ± 9	-144 ± 9	-144 ± 12

Table 3. Potential Energies and Heats of Adsorption in kJ/mol at Three Overall Compositions

System	Property	Composition 1000 : 9	1000 : 18	1000 : 36
Glucose in zeolite	U	−400	−409	−416
Water in zeolite	U	−29	−33	−35
Glucose adsorption	ΔH_{ads}	–108	–117	–124

in the gas phase and the $p\Delta V \approx RT$ contribution can be used to estimate the enthalpy of adsorption. Here, we find values ranging from −108 to −124 kJ/mol from the lowest to the highest glucose concentration. A simple molecular dynamics calculation on fully flexible D-glucose and fully flexible all-silica zeolite beta at $T = 343$ K with the DREIDING interatomic potential[39] gives a $\Delta U_{ads} = -130$ kJ/mol at a loading of four glucose per crystallographic unit cell. The ΔH_{ads} values found here are also comparable to the binding energy of −127 kJ/mol for unprotonated fructose in HZSM-5 estimated from periodic electronic structure calculations with dispersion correction.[40]

Using the values for the lowest concentration, because the infinite dilution case was used for ΔH_{sol}, these data can be applied to estimate the entropies of transfer of glucose, and we find −270 J/(mol K) for the transfer from the vapor phase to the zeolite and + 90 J/(mol K) for the transfer from the aqueous phase to the zeolite, that is, the entropy plays a significant role in aiding glucose to adsorb in the zeolite, but the Gibbs free energy is still unfavorable (see above). The ΔS_{trans} values are summarized in Table 4.

To provide further insight into the large and positive value of ΔS_{trans} for glucose from the aqueous solution to the vapor phase, the structure of the aqueous solution was analyzed. The oxygen(glucose)–oxygen(water) radial distribution functions (RDFs) for four representative systems are illustrated in Figure 2. The characteristically sharp peak centered at 0.28 nm is a good indication for the formation of strong hydrogen bonds, but the heights of the first peak are much lower than those found for oxygen(water)–oxygen(water) RDFs (not shown). Furthermore, the latter RDFs show a weak second peak at 0.44 nm for the second solvent shell of tetrahedrally coordinated water, but only a shoulder is found in this region for the oxygen(glucose)–oxygen(water) RDFs. Thus, the presence of the glucose solute leads to a significant disturbance of the local solvent structure. The fact that the oxygen(glucose)–oxygen(water) RDFs remain below unity up to 0.7 nm is likely due to the excluded volume of glucose. The oxygen(glucose)–oxygen(water) RDFs do not exhibit significant changes as temperature and composition are varied over the range of conditions studied here.

Additional insight about the solvation structure can be gleaned from a hydrogen bond analysis. In this work, a hydrogen bond was defined by either (loose) solely distance criteria of $r_{OH} < 0.25$ nm and $r_{OO} < 0.33$ nm, or (strict) a combination of the same distance criteria and an angular bound of $\cos\phi_{O\text{-}H\cdots O} < -0.4$, where the acceptor oxygen

Table 4. Transfer Entropies for Glucose in J/(mol K)

Process	ΔS_{trans}
Solution to vapor	+280 ± 20
Vapor to zeolite	−190 ± 20
Solution to zeolite	+90 ± 30

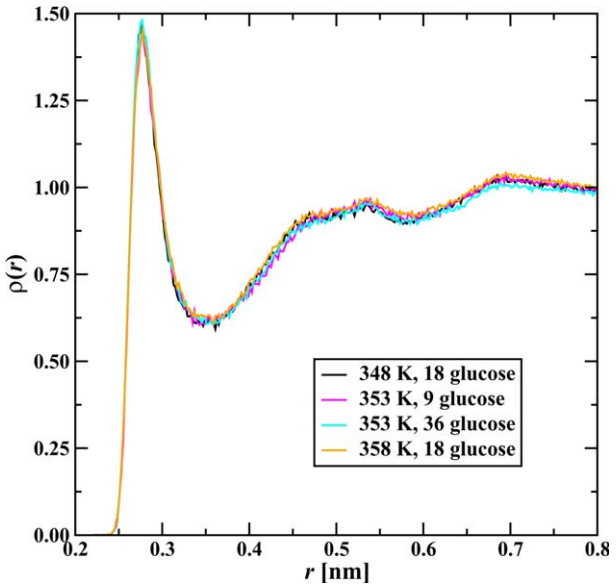

Figure 2. Oxygen(glucose)–oxygen(water) radial distribution function for selected systems.

[Color figure can be viewed in the online issue, which is available at wileyonlinelibrary.com.]

can be either from a water or glucose molecule or from the zeolite framework. Quantitative data on the number and type of hydrogen bonds are provided in Figure 3. For the conditions investigated here, there is not any significant concentration dependence for the number of hydrogen bonds being formed in the solution phase. Using the loose criteria, the glucose molecule in aqueous solution is involved in the formation of about 11 (intermolecular and intramolecular) hydrogen bonds. About six of these involve glucose as the acceptor and water as the donor, whereas about four of these involve glucose as the donor and water as the acceptor, that is, the hydroxyl groups of glucose are better hydrogen bond acceptors than donors. In solution, the number of intramolecular glucose–glucose hydrogen bonds is about one. In contrast, a glucose molecule in the gas phase forms about two hydrogen bonds at $T = 353$ K; that is, the conformational distribution of glucose changes on solvation. Using the strict criteria, the total number of hydrogen bonds is reduced to 10; with the largest decrease found for the intramolecular hydrogen bond. The observation that a glucose molecule is involved in about 10 hydrogen bonds (using either the loose or strict criteria) with solvation water at $T = 353$ K) agrees well with the results obtained from nuclear magnetic resonance spectra that each glucose hydroxyl group forms two hydrogen bonds to water (at $T = 273$ K).[41]

For the hydrogen bond analysis of water, the solvent molecules were grouped into those inside the first solvation shell of glucose, as defined by forming at least one hydrogen bond to a glucose molecule, and those outside the first solvation shell. Applying the present geometric criteria for hydrogen bond formation, water molecules are involved in about 3.7 hydrogen bonds that are equally divided between donor and acceptor interactions. Water molecules inside glucose's first solvation shell are found to act as donor and acceptor for about 0.7 and 0.5, respectively, hydrogen bonds with glucose. These values agree with the observation that glucose is the acceptor for more hydrogen bonds than it is the donor. Because glucose forms about 10 hydrogen bonds to

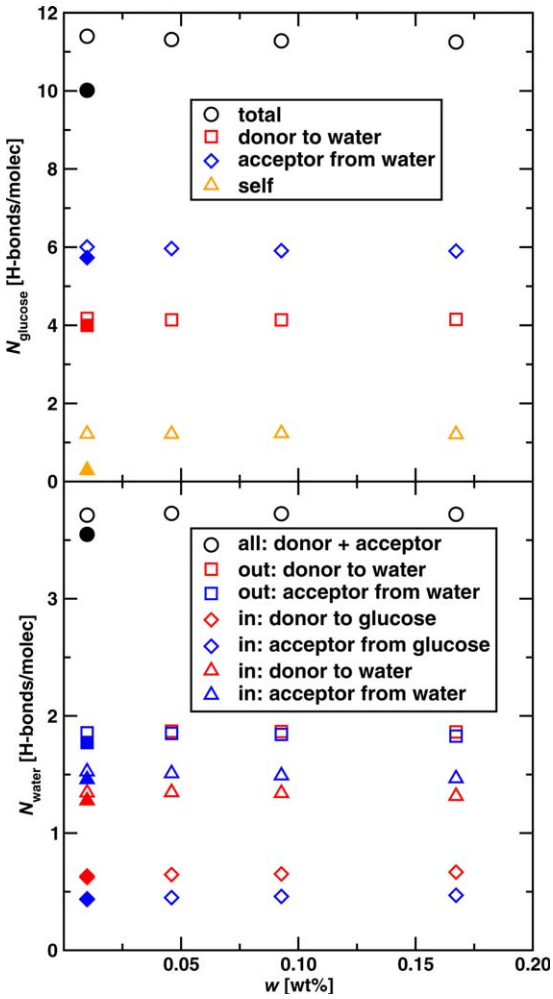

Figure 3. Number of hydrogen bonds for glucose (top) and water (bottom) molecules in the aqueous phase at $T = 353$ K.

The open and filled symbols show data computed with the loose and strict hydrogen bond criteria, respectively. (Top) The black circles, red squares, blue diamonds, and orange triangles show the number of hydrogen bonds of any type, with glucose as the donor and water as the acceptor, with glucose as the acceptor and water as the donor, and of intramolecular hydrogen bonds, respectively. (Bottom) The black circles, red squares, and blue squares show the number of hydrogen bonds of any type averaged over all water molecules, and with water as a donor and as acceptor for water molecules outside of the solvation shell of a glucose molecule. The red diamonds, blue diamonds, red triangles, and blue triangles show the number of hydrogen bonds for water molecules inside the solvation shell of a glucose molecule with water as the donor and glucose as the acceptor, with water as the acceptor and glucose as the donor, with water as the donor and acceptor to/from another water molecule, respectively. [Color figure can be viewed in the online issue, which is available at wileyonlinelibrary.com.]

hydration and the number of hydrogen bonds to glucose per water molecule is about 1.2, the number of hydrogen-bonded water molecules is 8–9. This value is somewhat higher than the number of six solvation water molecules deduced from dielectric relaxation studies.[42] The water molecules inside the first solvation shell are also found to act as donor and as acceptor for about 1.3 and 1.5 hydrogen bond from other water molecules. The total number of hydrogen bonds per water molecule is slightly higher for molecules in the first solvation shell than outside of it. As also observed for the RDFs, the formation of hydrogen bonds in the aqueous solution does not depend significantly on the state point.

To provide further insight into the concentration dependence of the enthalpy of adsorption, the distribution of the potential energies for glucose and water in the zeolite were analyzed. Figure 4 shows the distributions for glucose for four representative systems. The temperature dependence is very small, but increasing the overall number of glucose molecules and correspondingly the loading of glucose shifts the distribution to lower energies. It should be noted here that the potential energy of a vapor-phase glucose molecule is about −295 kJ/mol and that this value needs to be subtracted from the potential energies of adsorbed glucose molecules to obtain ΔH_{ads}. Because the zeolite is treated in this work as rigid, there is no contribution from changes in the zeolite configuration. The number of hydrogen bonds per glucose molecule with other sorbate molecules is found to increase from about 0.5 for the lowest concentration to about 1 for the highest concentration, whereas the number of intramolecular hydrogen bonds remains close to 1.2 for all three compositions. To illustrate the packing of glucose in zeolite beta, a snapshot is shown in Figure 5. As can be seen, the fit of the glucose molecule is relatively tight and the molecular long axis is aligned with the channel direction.

The distributions of the potential energies for adsorbed water molecules are illustrated in Figure 6. In this case, the composition dependence is more significant. The energy distribution for water is bimodal with the sharper peak at −10 kJ/mol reflecting water molecules that interact only with the zeolite framework, and the broader peak at more favorable energies is caused by water molecules forming at least one hydrogen bond with other sorbate molecules. At the lower glucose concentration, the nonhydrogen-bonding peak is higher, but its integral smaller than for the hydrogen-bonding peak. At the highest glucose concentration, the nonhydrogen-

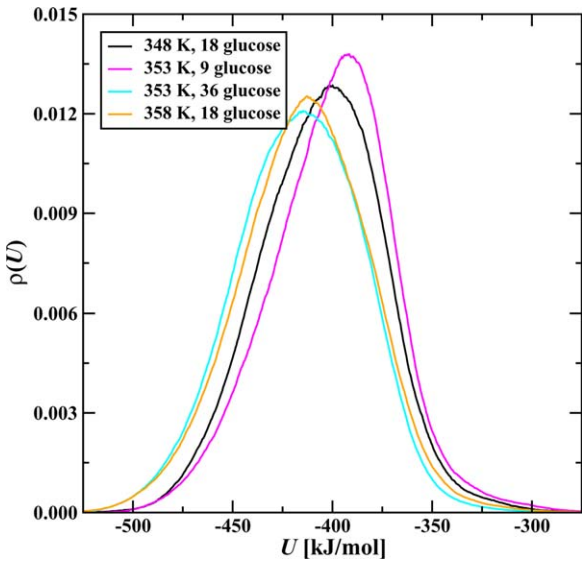

Figure 4. Adsorption energy distributions for glucose in all-silica zeolite beta for four selected systems.

For the 18-glucose molecule system, the loadings were 0.29 and 0.37 per unit cell at $T = 348$ K and 358 K, respectively. [Color figure can be viewed in the online issue, which is available at wileyonlinelibrary.com.]

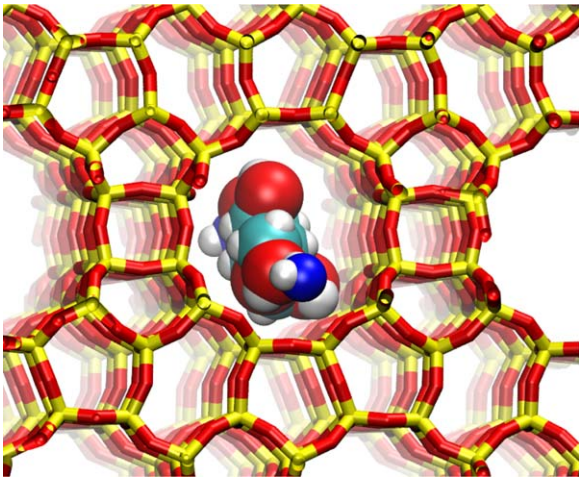

Figure 5. Snapshot of glucose molecule in all-silica zeolite beta.

[Color figure can be viewed in the online issue, which is available at wileyonlinelibrary.com.]

bonding peak is greatly diminished, whereas the hydrogen-bonding peak increases and shifts to more favorable energies. The somewhat larger number of glucose molecules adsorbed in the zeolite found for the 18-molecule system at 358 K is likely responsible for the larger fraction of water molecules with more favorable interaction energies compared to the 18-molecule system at 348 K. The number of hydrogen bonds per water molecule with other sorbate molecules is found to increase from about 0.7 for the lowest concentration to about 1 for the highest concentration.

The oxygen(glucose)–oxygen(zeolite) RDFs for selected systems are shown in Figure 7. As expected for a hydrophobic all-silica framework and from the relatively small magnitude of the adsorption energy for water molecule interacting only with the zeolite framework, see Figure 6, the RDFs show only a weak shoulder in the typical hydrogen bond region. Neither concentration, that is, glucose loading, nor temperature has a significant effect on these RDFs.

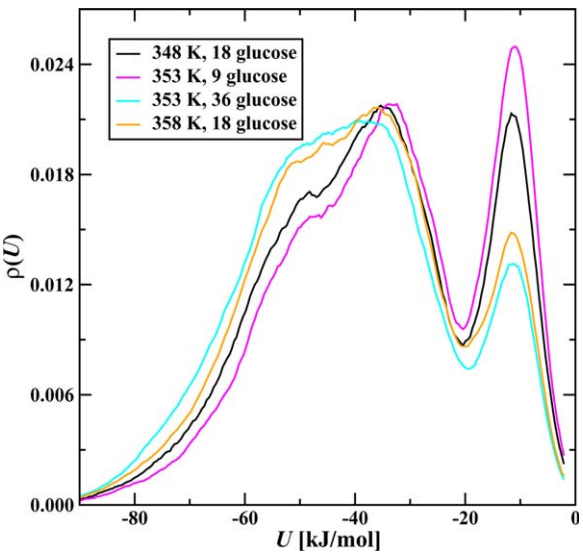

Figure 6. Adsorption energy distributions for water in all-silica zeolite beta for four selected systems.

[Color figure can be viewed in the online issue, which is available at wileyonlinelibrary.com.]

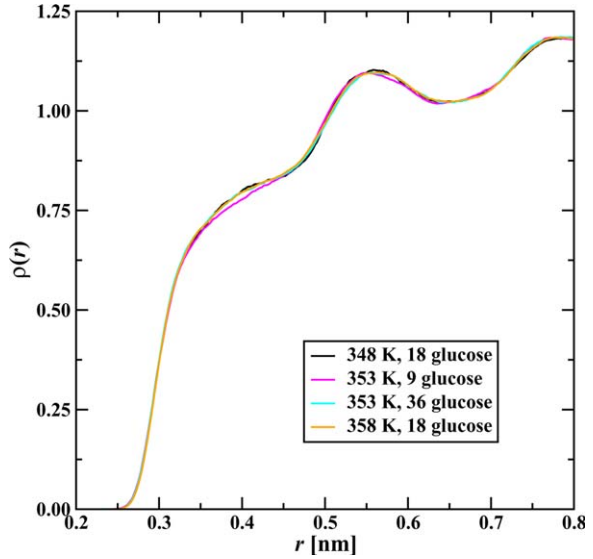

Figure 7. Oxygen(glucose)–oxygen(zeolite) radial distribution functions.

[Color figure can be viewed in the online issue, which is available at wileyonlinelibrary.com.]

Conclusions

As shown in Table 4, the solvation entropy of glucose is negative. Both reconfiguration of the water molecules around the glucose and change in the glucose conformational distribution function contribute to this solvation entropy. Because the average number of hydrogen bonds per water molecules in the first coordination shell of glucose is 4.3, greater than the 3.7 per bulk water molecule, it would appear that water is more constrained around glucose relative to bulk water. These results are consistent with previous observations of increased water densities around glucose.[43–45] Removing the glucose reduces this constrained structure, and so it would appear that there is an entropic force to drive glucose out of solution. Glucose may be more conformationally restricted in the gas phase, as measured by the two intramolecular hydrogen bonds formed, than in the liquid phase, as measured by the one intramolecular hydrogen bond formed. If so, this result along with the negative entropy of solvation also indicates an entropic water unstructuring force to drive glucose out of solution. Finally, and alternatively, we may argue that because there are few conformational degrees of freedom in glucose, the majority of the + 280 J/(mol K) entropy of transfer from solution to vapor must be due to water unstructuring.

The free energy of transfer for glucose from solution to zeolite beta is the sum of the entropic, water-restructuring contribution, and the enthalpy of transfer, as $\Delta G_{\text{trans}} = \Delta H_{\text{trans}} - T\Delta S_{\text{trans}}$. For all-silica zeolite beta, the enthalpy of transfer is rather unfavorable. Nonetheless, there is a measurable loading of glucose in the zeolite, due to the compensating entropy of transfer. Significantly, the transfer of glucose from aqueous solution to the zeolite reduces the extensive hydration of aqueous glucose to a single water molecule coadsorbed per glucose molecule in the zeolite. The exclusion of bulk water is a key feature in the mechanism of glucose isomerization in hydrophobic zeolites.[15] The metal binding sites in Ti- or Sn-beta may favorably enhance the enthalpy of transfer for glucose and may increase the substrate loading of glucose for isomerization in these

Lewis acid zeolites. Temperature-programmed desorption experiments on Sn or Ti beta[16] in 1 wt % glucose solution suggest the glucose loading in these materials is 5–10 times larger than that extrapolated from the present calculations for all-silica beta.

Acknowledgment

This research was supported by the U.S. Department of Energy, Office of Basic Energy Sciences, Division of Chemical Sciences, Geosciences and Biosciences, under awards DE-FG02-03ER15456 and DE-FG02-12ER16362.

Literature Cited

1. Sherman JD. Synthetic zeolites and other microporous oxide molecular sieves. *Proc Natl Acad Sci USA*. 1999;96:3471–3478.
2. Davis ME. Ordered porous materials for emerging applications. *Nature*. 2002;417:813–821.
3. Davis ME. Reaction chemistry and reaction-engineering principles in catalyst design. *Chem Eng Sci*. 1994;49:3971–3980.
4. Flanigen EM, Patton RL. Silica polymorph and process for preparing the same. US Patent 4,073,865. 1978.
5. Flanigen EM, Bennett JM, Grose RW. Silicalite, a new hydrophobic crystalline silica molecular-sieve. *Nature*. 1978;271:512–516.
6. da Silva CXA, Goncalves VLC, Mota CJA. Water-tolerant zeolite catalyst for the acetalization of glycerol. *Green Chem*. 2009;11:38–41.
7. Moliner M, Román-Leshkov Y, Davis ME. Tin-containing zeolites are highly active catalysts for the isomerization of glucose in water. *Proc Natl Acad Sci USA*. 2010;107:6164–6168.
8. Zapata PA, Faria J, Ruiz MP, Jentoft RE, Resasco DE. Hydrophobic zeolites for biofuel upgrading reactions at the liquid-liquid interface in water/oil emulsions. *J Am Chem Soc*. 2012;134:8570–8578.
9. Nikolla E, Román-Leshkov Y, Moliner M, Davis ME. "One-pot" synthesis of 5-(hydroxymethyl)furfural from carbohydrates using tin-beta zeolite. *ACS Catal*. 2011;1:408–410.
10. Camblor MA, Corma A, Iborra S, Miquel S, Primo J, Valencia S. Beta zeolite as a catalyst for the preparation of alkyl glucoside surfactants: the role of crystal size and hydrophobicity. *J Catal*. 1997;172:76–84.
11. Choudhary V, Pinar A, Sandler SI, Vlachos DG, Lobo RF. Xylose isomerization to xylulose and its dehydration to furfural in aqueous media. *ACS Catal*. 2011;1:1724–1728.
12. Román-Leshkov Y, Moliner M, Labinger JA, Davis ME. Mechanism of glucose isomerization using a solid acid catalyst in water. *Angew Chem Int Ed Engl*. 2010;49:8954–8957.
13. Lew CM, Rajabbeigi N, Tsapatsis M. Tin-containing zeolite for the isomerization of cellulosic sugars. *Microporous Mesoporous Mater*. 2012;153:55–58.
14. Bermejo-Deval R, Gounder R, Davis ME. Framework and extraframework tin sites in zeolite beta react glucose differently. *ACS Catal*. 2012;2:2705–2713.
15. Bermejo-Deval R, Assary RS, Nikolla E, Moliner M, Román-Leshkov Y, Hwang SJ, Palsdottir A, Silverman D, Lobo RF, Curtiss LA, Davis ME. Metalloenzyme-like catalyzed isomerizations of sugars by Lewis acid zeolites. *Proc Natl Acad Sci USA*. 2012;109:9727–9732.
16. Gounder R, Davis ME. Beyond shape selective catalysis with zeolites: hydrophobic void spaces in zeolites enable catalysis in liquid water. *AIChE J*. http://dx.doi.org/10.1002/aic.14016.
17. Newsam JM, Treacy MMJ, Koetsier WT, de Gruyter CB. Structural characterization of zeolite-beta. *Proc R Soc London A*. 1988;420:375–420.
18. Jorgensen WL, Chandrasekhar J, Madura JD, Impey RW, Klein ML. Comparison of simple potential functions for simulating liquid water. *J Chem Phys*. 1983;79:926–935.
19. Damm W, Frontera A, Tirado-Rives J, Jorgensen WL. OPLS all-atom force field for carbohydrates. *J Comput Chem*. 1997;18:1955–1970.
20. Bai P, Tsapatsis M, Siepmann JI. Multicomponent adsorption of alcohols onto silicalite-1 from aqueous solution: isotherms, structural analysis, and assessment of ideal adsorbed solution theory. *Langmuir*. 2012;28:15566–15576.
21. Siepmann JI, et al. Transferable potentials for phase equilibria force field. Accessed in November 2012. http://www.chem.umn.edu/groups/siepmann/trappe/intro.php.
22. Allen MP, Tildesley DJ. Computer Simulation of Liquids. Oxford University Press, Oxford, 1987.
23. June RL, Bell AT, Theodorou DN. Prediction of low occupancy sorption of alkanes in slicalite. *J Phys Chem*. 1990;94:1508–1516.
24. Siepmann JI, et al. Monte Carlo for complex chemical systems, Version 2012-1. Minnesota. Accessed in November 2012. Available at http://www.chem.umn.edu/groups/siepmann/software.html.
25. Panagiotopoulos AZ, Quirke N, Stapleton M, Tildesley DJ. Phase-equilibria by simulation in the Gibbs ensemble—alternative derivation, generalization and application to mixture and membrane equilibria. *Mol Phys*. 1988;63:527–545.
26. Chen B, Siepmann JI. Microscopic structure and solvation in dry and wet octanol. *J Phys Chem B*. 2006;110:3555–3563.
27. Rafferty JL, Zhang L, Siepmann JI, Schure MR. Retention mechanism in reversed-phase liquid chromatography: a molecular perspective. *Anal Chem*. 2007;79:6551–6558.
28. Siepmann JI, Frenkel D. Configurational bias Monte-Carlo—a new sampling scheme for flexible chains. *Mol Phys*. 1992;75:59–70.
29. Mooij GCAM, Frenkel D, Smit B. Direct simulation of phase equilibria of chain molecules. *J Phys: Condens Matter*. 1992;4:L255–L259.
30. Laso M, de Pablo JJ, Suter UW. Simulation of phase equilibria for chain molecules. *J Chem Phys*. 1992;97:2817–2819.
31. Martin MG, Siepmann JI. Novel configurational-bias Monte Carlo method for branched molecules. Transferable potentials for phase equilibria. 2. United-atom description of branched alkanes. *J Phys Chem B*. 1999;103:4508–4517.
32. Martin MG, Siepmann JI. Predicting multicomponent phase equilibria and free energies of transfer for alkanes by molecular simulation. *J Am Chem Soc*. 1997;119:8921–8924.
33. Rafferty JL, Siepmann JI, Schure MR. Retention mechanism for polycyclic aromatic hydrocarbons in reversed-phase liquid chromatography with monomeric stationary phases. *J Chromatogr A*. 2011;1218:9183–9193.
34. McDonald IR. NpT-ensemble Monte Carlo calculations for binary liquid mixtures. *Mol Phys*. 1972;23:41–58.
35. Zhao Y, Truhlar DG. The M06 suite of density functionals for main group thermochemistry, thermochemical kinetics, noncovalent interactions, excited states, and transition elements: two new functionals and systematic testing of four M06-class functionals and 12 other functionals. *Theor Chem Acc*. 2008;120:215–241.
36. Bai P, Siepmann JI. Selective adsorption from dilute solutions: Gibbs ensemble Monte Carlo simulations. *Fluid Phase Equilib*. http://dx.doi.org/10.1016/j.fluid.2012.08.014.
37. Martin MG, Siepmann JI. Calculating Gibbs free energies of transfer from Gibbs ensemble Monte Carlo simulations. *Theor Chem Acc*. 1998;99:347–350.
38. Wick CD, Siepmann JI, Schure MR. Temperature dependence of transfer properties: importance of heat capacity effects. *J Phys Chem B*. 2003;107:10623–10627.
39. Mayo SL, Olafson BD, Goddard WA. DREIDING: A generic force-field for molecular simulations. *J Phys Chem B*. 1990;94:8897–8909.
40. Cheng L, Curtiss LA, Assary RS, Greeley J, Kerber T, Sauer J. Adsorption and diffusion of fructose in zeolite HZSM-5: selection of models and methods for computational studies. *J Phys Chem C*. 2011;115:21785–21790.
41. Harvey JM, Symons MCR, Naftalin RJ. Proton magnetic resonance study of hydration of glucose. *Nature*. 1976;261:435–436.
42. Franks F, Reid DS, Suggett A. Conformation and hydration of sugars and related compounds in dilute aqueous solution. *J Solution Chem*. 1973;2:99–118.
43. Gallina ME, Sassi P, Paolantoni M, Morresi A, Cataliotti RS. Vibrational analysis of molecular interactions in aqueous glucose solutions. Temperature and concentration effects. *J Phys Chem B*. 2006;110:8856–8864.
44. Paolantoni M, Sassi P, Morresi A, Santini S. Hydrogen bond dynamics and water structure in glucose-water solutions by depolarized Rayleigh scattering and low-frequency Raman spectroscopy. *J Chem Phys*. 2007;127:024504.
45. Lee SL, Debenedetti PG, Errington JR. A computational study of hydration, solution structure, and dynamics in dilute carbohydrate solutions. *J Chem Phys*. 2005;122:204511.

Manuscript received Dec. 26, 2012, and revision received Feb. 18, 2013.